Wet thermal oxidation of AlAsSb alloys lattice matched to GaSb

K. Meneou, H. C. Lin, K. Y. Cheng, J. G. Kim, and R. U. Martinelli

Citation: J. Appl. Phys. **95**, 5131 (2004); doi: 10.1063/1.1687976

View online: http://dx.doi.org/10.1063/1.1687976

View Table of Contents: http://jap.aip.org/resource/1/JAPIAU/v95/i9

Published by the American Institute of Physics.

Wet thermal oxidation of AlAsSb alloys lattice matched to GaSb

K. Meneou, H. C. Lin, and K. Y. Cheng[a)]
Department of Electrical and Computer Engineering, and Micro and Nanotechnology Laboratory, University of Illinois at Urbana-Champaign, Urbana, Illinois 61801

J. G. Kim and R. U. Martinelli
Sarnoff Corporation, CN5300, Princeton, New Jersey 08543-5300

(Received 6 October 2003; accepted 28 January 2003)

Lateral wet oxidation of thin (1000 Å) films of $AlAs_{0.1}Sb_{0.9}$ was performed at temperatures ranging from 300 to 450 °C. Oxidation kinetics and morphology were studied to assess the utility of an $AlAs_{0.1}Sb_{0.9}$ oxidation process. Oxidation rates up to 2.15 μm/min and maximum oxidation depths up to 130 μm were achieved at temperatures below 350 °C. The oxidation starts out reaction rate limited, becoming diffusion rate limited at longer oxidation times and higher oxidation temperatures. At higher temperatures, the apparent diffusion constant decreases, limiting maximum oxide depth in a phenomenon called self-limiting oxidation, as has also been observed during oxidation of $AlAs_{0.56}Sb_{0.44}$. Surface and oxidation front morphology are studied to help understand the transport of reactants through the oxide. Composition and structure of the oxide are studied to shed more light on the oxidation kinetics. In particular, we suggest a physical explanation for how self-limiting oxidation occurs in this material. © *2004 American Institute of Physics.*
[DOI: 10.1063/1.1687976]

I. INTRODUCTION

Lateral oxidation of $Al_xGa_{1-x}As$ has been studied extensively in the last 15 years because of useful properties such as high oxidation rate at low temperatures, excellent selectivity with respect to GaAs, and an oxide of good optical quality.[1] This process has been used for current confinement in heterojunction bipolar transistors,[2] for lattice engineering to allow growth of InGaAs on GaAs with lower defect density,[3] and for achieving lower threshold currents in vertical cavity surface emitting lasers.[4] Following the increased exploration of the InP material system, there have been several reports on lateral oxidation of $AlAs_xSb_{1-x}$ ($x=0.56$) lattice matched to InP in the last several years.[5–12] The material has a high oxidation rate at low temperatures and good selectivity to some InP-based materials, and so could fill a similar role in the InP system that AlGaAs oxidation fills in the GaAs system. There have been some concerns about its optical quality due to numerous reports of the formation of a segregated Sb layer at the interfaces of the oxidized layer,[5,11] but recently it was discovered that the Sb layer can be eliminated by adding a small amount of Ga ($Al_{0.95}Ga_{0.05}As_{0.56}Sb_{0.44}$).[6] Compositions of AlAsSb other than $AlAs_{0.56}Sb_{0.44}$ have been studied in detail,[7] but not with Sb>0.50. The case of $AlAs_xSb_{1-x}$ ($x=0.1$) lattice matched to GaSb is particularly interesting. It is known to have a fairly high oxidation rate at low temperatures, but it has only been lightly studied,[8] and could become an interesting processing option in future GaSb system devices. In this article, we present data on oxidation kinetics, oxide structure, and oxide morphology of $AlAs_{0.1}Sb_{0.9}$ in order to determine the optimal oxidation conditions.

a)Electronic mail: k-cheng@uiuc.edu

II. EXPERIMENT

Samples were grown by molecular beam epitaxy. Epitaxial growth was performed on (100) *n*-type GaSb substrates. First, a 100 nm thick layer of $AlAs_{0.1}Sb_{0.9}$ was grown, followed by a 100 nm thick cap layer of GaSb. The GaSb cap is thick enough to prevent oxidation of $AlAs_{0.1}Sb_{0.9}$ through the cap, but thin enough so that the progress of oxidation is visible with an optical microscope through the cap.

Samples were oxidized in a 5 cm diameter open quartz tube, single zone furnace. The carrier gas, dry N_2, was flowed into a bubbler at the rate of 0.9 slm and then into the furnace. The bubbler contained deionized water heated to 85–86.5 °C. Samples were cleaved into squares to expose the $AlAs_{0.1}Sb_{0.9}$ layer immediately before loading them into the furnace.

Oxidation progress was measured from Nomarski optical micrographs of the sample surface. Morphology of the oxidation was studied using optical microscopy and using a Dimension 3100 atomic force microscope (AFM). A Hitachi S-4700 scanning electron microscope (SEM) was used to take cross-sectional scanning electron micrographs to look at the structure of the oxidized layer and measure the change in thickness of the $AlAs_{0.1}Sb_{0.9}$. Auger depth profiling was performed with a Physical Electronics PHI 660 Scanning Auger Microprobe.

III. RESULTS

Optical microscopy showed that the oxidation front took on two distinct shapes: smooth and straight at lower temperatures and shorter oxidation times, changing to a dendritic front at longer oxidation times and higher temperatures. The evolution of the dendrites, or fingers, is shown in Fig. 1 and is described as follows: growth of the smooth front continues

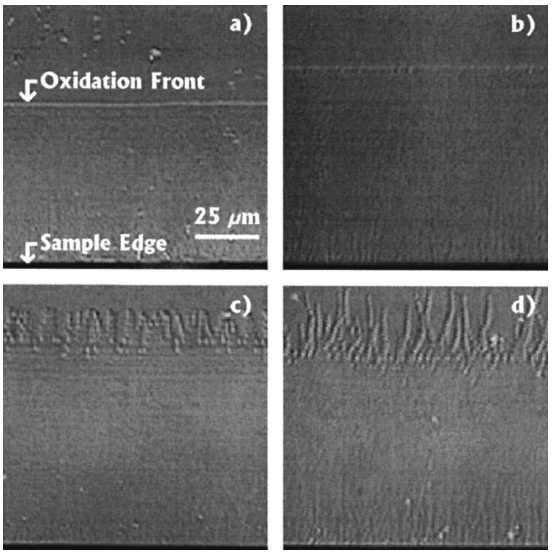

FIG. 1. Nomarski micrographs of four different samples oxidized at 340 °C showing the evolution of the fingers. Scale is the same for all micrographs: (a) 45 min oxidation time, front is still smooth and straight; (b) 60 min, chinks develop in oxidation front that will form the base of fingers; (c) 90 min, oxidation does not occur in the chinks, creating fingers. The oxidation front at the tips of the fingers is still flat; and (d) 120 min, fingers become pointy as they grow longer and skinnier.

until some critical oxidation time when small chinks or crevices appear along the oxidation front, the first sign of fingers. Oxidation stops at the chinks, dividing the front into fingers; then the fingers get thinner and more pointy as they lengthen with further oxidation.

Looking at the oxidation kinetics will give us additional insight about the oxidation front morphology. On the samples with smooth, straight oxidation fronts, measuring oxide depth is simple. However, on the samples with dendritic oxidation fronts, oxidation depth could be measured either to the base of the fingers or to the tips of the fingers. We focus on the measurement to the base of the fingers as the figure of greater technological interest. On the plots that follow, the oxide depth is taken as the depth to the base of the fingers. However, on samples where fingers occurred, the additional length of the fingers is indicated by an error bar. Measurements of oxidation depth were taken on all four sides of a cleaved sample and averaged to obtain the final oxide depth for that sample.

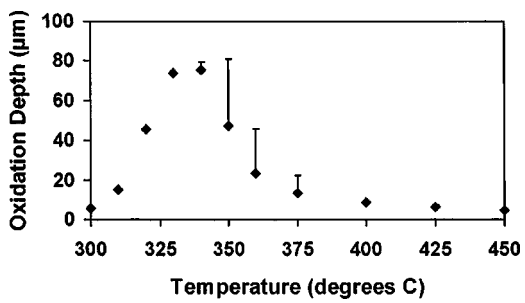

FIG. 2. Oxidation depth as a function of temperature for oxidation time of 60 min. The error bars indicate the additional length of the fingers, where they occur.

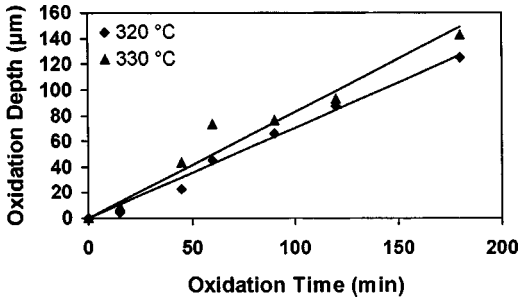

FIG. 3. Oxidation depth as a function of oxidation time at 320 and 330 °C. No fingers occurred at these low oxidation temperatures.

First, to examine oxidation rate variation with temperature, oxidation was performed for 60 min at temperatures ranging from 300–450 °C. The results are shown in Fig. 2. For this oxidation time of 60 min, fingers formed on all samples oxidized at over 330 °C. They are longest at 350–375 °C. They form at higher temperatures ($\geqslant$400 °C) but become very short and difficult to measure. The plot indicates an appreciable oxidation rate was achieved at the relatively low temperatures 330–340 °C. From this plot, we further selected 320, 330, 340, 350, and 375 °C as the temperatures of greatest interest at which we would study oxidation kinetics.

At these temperatures, oxidation time was ranged from 15 to 180 min and plots of oxidation depth versus oxidation time prepared. The plots for 320 and 330 °C are shown in Fig. 3. The plots are linear, indicating reaction rate limited oxidation at these temperatures for all oxidation times tested. Experiments with higher gas flow rates in the furnace did not result in deeper oxidation so that reactant-limited oxidation can be ruled out. From the slope of the lines, the oxidation rate at 330 °C is the higher of the two, approximately 0.82 μm/min. Only smooth oxidation fronts were observed at these low temperatures.

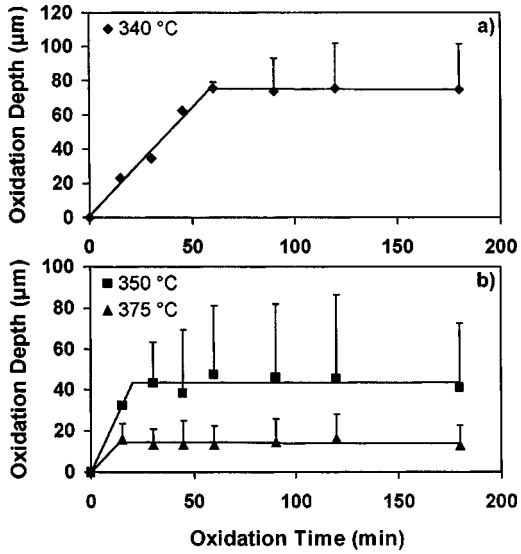

FIG. 4. Oxidation depth as a function of oxidation time at (a) 340 °C, and (b) 350 and 375 °C. The error bars indicate the additional length of the fingers, where they occur.

Fingers occur at higher oxidation temperatures. Figures 4(a) and 4(b) show the oxide depth for 340, 350, and 375 °C as a function of oxidation time. Fingers appear sooner at higher oxidation temperatures, first appearing at 60, 30, and 15 min oxidation time for 340, 350, and 375 °C, respectively. Before the fingers appear, the oxidation is reaction rate limited (linear). The slopes of the lines indicate a reaction rate of 1.29 μm/min at 340 °C and a rate of 2.15 μm/min at 350 °C, the highest oxidation rate recorded in this study. Thus, the reaction rate monotonically increases as temperature increases from 320 to 350 °C. However, at longer oxidation times fingers form, and reaction rate limited oxidation ends. After the fingers form, further oxidation can cause the tips of the fingers (tops of the error bars) to move further into the sample in a sublinear manner, but the base of the fingers (data points) will not move in any further.

We believe that the appearance of fingers marks the onset of diffusion limited oxidation in this material, in the sense that the deviation from reaction rate limited oxidation is caused by insufficient reactants available due to slower diffusion. Consider that in other studies of both AlAs (Ref. 13) and $AlAs_{0.56}Sb_{0.44}$,[9] diffusion limited oxidation occurred at higher oxidation temperatures and longer oxidation times, as here. In addition, similar dendritic oxidation front morphology has been observed after wet thermal oxidation of $AlAs_{0.56}Sb_{0.44}$;[10] in that report, the appearance of fingers was encouraged when less steam was available for reaction due to a higher methanol:water ratio through which the carrier gas was bubbled. We conclude that the formation of fingers here is probably an indication of transition to diffusion limited oxidation. Diffusion limited oxidation apparently can be manifested in $AlAs_{0.1}Sb_{0.9}$ and $AlAs_{0.56}Sb_{0.44}$, unlike in AlAs, by a change in the oxidation front morphology as well as a change in the oxidation kinetics.

Study of surface morphology of the oxidized region using optical microscopy and AFM revealed interesting formations of ridges in the oxidized region. The ridges run in from the edge roughly perpendicular to the edge, and are reminiscent of the morphological ordering described for oxidation of $AlAs_{0.56}Sb_{0.44}$, but are not as precisely aligned to the crystal direction.[9] The ridges were due to nonuniform thickness of the oxidized layer, which deforms the cap layer and can be detected by AFM on the surface. They were roughly 1–3 μm apart and 15–40 nm high and become larger and well ordered at low oxidation temperatures. Figure 5 shows an AFM image of a low temperature sample, oxidized at 320 °C for 90 min. The ridges at this temperature take on a fractal-like morphology in filling the space of the oxidized region. Figure 5 also demonstrates that anisotropic diffusion is occurring, and that the transport of reactants and/or products corresponds to the morphology of the ridges. The ridges become too disordered and hard to study at oxidation temperatures higher than 320 °C.

Auger depth profiling and cross-sectional SEM were used to study the composition and structure of the oxidized region. Auger depth profiling results for a sample oxidized at 375 °C for 60 min are shown in Fig. 6. Previous studies of $AlAs_{0.56}Sb_{0.44}$ show that the oxidized layer for that material consists of mostly AlO_x and elemental Sb.[5,11] Most of the As

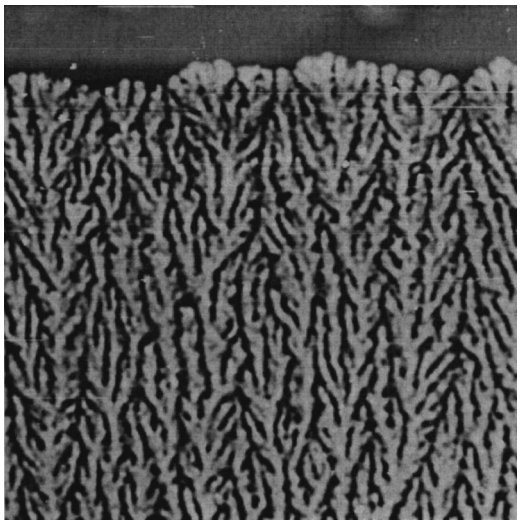

FIG. 5. AFM image of the surface of a GaSb–$AlAs_{0.10}Sb_{0.90}$–GaSb sample oxidized at 320 °C for 90 min. Oxidation proceeds from the bottom of the image. The image is 50 μm on a side. The ridges in the oxidized region have ~35 nm amplitude.

leaves the oxide as AsH_3, whereas most of the Sb remains due to SbH_3 being comparatively more difficult to form and having a much lower vapor pressure than AsH_3.[11] We expected that increasing the antimony content in AlAsSb would not affect the composition of the oxidized region (except that it will contain proportionally more Sb than $AlAs_{0.56}Sb_{0.44}$); Fig. 6(b) confirms the expected elemental composition of oxidized $AlAs_{0.1}Sb_{0.9}$. Figure 6 also shows weak segregation of materials within the oxidized layer, with more Sb in the center of the $AlAs_{0.1}Sb_{0.9}$ layer and more AlO_x at the interfaces with the cap and substrate. Looking just within the oxidized layer, the peaks and troughs of the O curve closely follow those of the Al curve but do not match up at all with the Sb curve, suggesting that the Al exists mainly as AlO_x

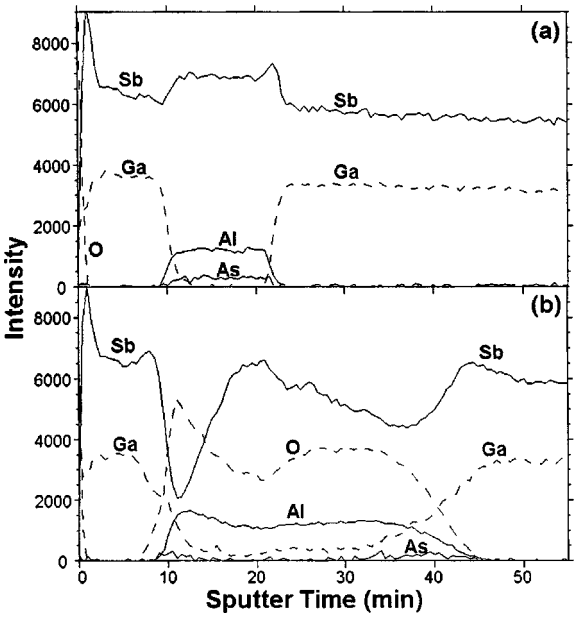

FIG. 6. Auger depth profiles from the (a) unoxidized and (b) oxidized regions of a GaSb–$AlAs_{0.10}Sb_{0.90}$–GaSb sample oxidized at 375 °C for 60 min.

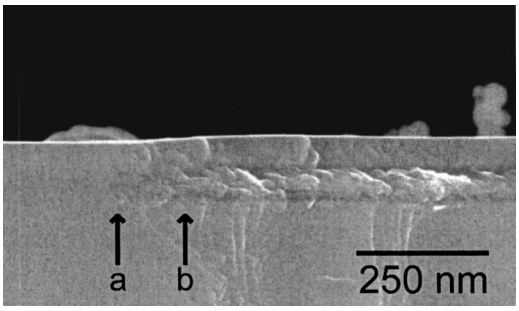

FIG. 7. Cross-sectional SEM micrographs of oxidation front region of a GaSb–$AlAs_{0.10}Sb_{0.90}$–GaSb sample oxidized at 375 °C for 60 min. Oxidation proceeds from the right side of the image. The oxidation front is at mark ''a.'' The transition region near the oxidation front where the segregation of materials breaks down is between marks ''a'' and ''b.'' The dark material at the top and bottom interfaces of the $AlAs_{0.10}Sb_{0.90}$ is AlO_x and the bright colored material in the $AlAs_{0.10}Sb_{0.90}$ layer is elemental Sb.

and the Sb exists mainly as elemental Sb. Finally, we note that the transitions at the interfaces of the oxidized layer are not very sharp compared to the depth profile for the unoxidized region, indicating a mixing of materials from the oxidized layer with materials from the cap layer and, especially, the substrate. In particular, oxidation results in a high concentration of Ga contamination through the whole oxidized layer.

Figure 7 shows a cross-sectional SEM micrograph of the region near the oxidation front for a sample oxidized at 375 °C for 60 min. The oxidation looks inhomogeneous and grainy, with bits of light and dark colored material mixed together. Note first that no distinct bright, segregated Sb layer forms at the interfaces of the oxidized layer as for $AlAs_{0.56}Sb_{0.44}$. Still, some segregation of materials in the oxide layer is evident: The oxidized layer is darker in color near the interfaces with the cap and substrate and brighter in the middle. Comparing with Fig. 6(b), we conclude that the darker material is AlO_x and the brighter material is mostly elemental Sb. The Sb appears to form large grains in the center of the oxide. This segregation of material into layers occurred only at temperatures above 375 °C; segregation of the Sb and AlO_x occurred at low temperatures, but grains of the two materials were spread randomly through the oxide, with no layered ordering. SEM measurements show that the $AlAs_{0.1}Sb_{0.9}$ layer swells ~15–25% during oxidation, comparable to the swelling reported for $AlAs_{0.56}Sb_{0.44}$.[5,9] There is a transition region visible in Fig. 7 extending laterally from the oxidation front to several hundred nanometers behind the oxidation front that interfaces between the fully swollen oxide and the 1000 Å thick unoxidized $AlAs_{0.1}Sb_{0.9}$. In this region, which has not swelled to its full thickness yet but is clearly oxidized, the segregation of materials into layers seen further back from the oxidation front breaks down. It is unclear what the composition or structure of this transition region is, but it is clearly different from the rest of the oxidized layer further behind the oxidation front. Furthermore, the transition region is only visible by SEM in samples oxidized at 375 °C and above, and grows wider and more distinct with increasing temperature. A thin transition region behind the oxidation front with different structure and composition than the rest of the oxide such as this is similar to a structural feature reported for $AlAs_{0.56}Sb_{0.44}$, where the segregated Sb layer lagged the oxidation front's progress by hundreds of nanometers.[9] Finally, as far as selectivity to GaSb is concerned, it is worth noting that oxidation of the GaSb cap surface was visible in SEM at higher temperatures (not shown), with 35 nm of oxidation measured on a sample oxidized at 375 °C for 100 min. Furthermore, roughening of the $AlAs_{0.1}Sb_{0.9}$ interfaces with the GaSb cap and substrate that appeared to be oxidation of the cap and substrate outward from the oxidized $AlAs_{0.1}Sb_{0.9}$ layer could be seen at higher temperatures (above 375 °C and above 100 min oxidation time; not shown). Such roughening of the layer interfaces was quite shallow (about 8 nm for 60 min oxidation at 425 °C) and so does not much compromise the selectivity of this process to GaSb, but is deep enough to account for the gradual transitions at the interfaces of the oxidized layer shown in Fig. 6(b).

IV. DISCUSSION

In light of the composition and structure of the oxide, the reason the fingers form is still not entirely clear. In particular, cross-sectional SEM of the fingers themselves (not shown) reveals no structural differences on the sides of the fingers that would inhibit oxidation out from the sides of the fingers. Generally speaking, it seems the anisotropic oxidation resulting in fingers must be attributable to anisotropic diffusion of reactants and/or the inhomogeneous structure of the oxide as shown by Figs. 5 and 7, respectively; neither of which condition is the case for oxidation of AlAs. No explicit correlation between the locations of the ridges as shown in Fig. 5 and the fingers could be established because the ridges are too faint to study at oxidation temperatures high enough for fingers to form. We suspect the thickness of the $AlAs_{0.1}Sb_{0.9}$ layer may also influence the formation of fingers.

We can better explain Fig. 2 in terms of what we know about the structure of the oxidized layer. In terms of what we have learned about oxidation kinetics, the plot is simple to understand from 300 to 330 °C: the oxidation (reaction) rate increases in a roughly exponential manner with increasing temperature. This is precisely what was observed for AlAs.[14] At 340 °C and above, the exponential growth trend abruptly stops and the oxidation depth decays down to zero for higher temperatures. This behavior was encountered by S. K. Mathis *et al.* in $AlAs_{0.56}Sb_{0.44}$ and termed ''self-limiting'' oxidation.[9] They reported that at temperatures greater than 450 °C, the apparent diffusion constant went quickly to zero, resulting in shallower oxidation at higher temperatures. Oxidation kinetics data at 350 and 375 °C in Fig. 4 shows that reaction rates achieved over the first 15 min of oxidation at 350 and 375 °C are higher than the reaction rates found for 340 °C, so that the reaction rate continues to increase with oxidation temperature. Instead, slower and earlier onset diffusion limited oxidation with increasing temperature, or self-limiting oxidation, cause the shallower oxidation with increasing temperature.

The model proposed by Mathis *et al.* to explain self-limiting oxidation in $AlAs_{0.56}Sb_{0.44}$ involved an Sb-rich in-

terfacial layer (''reaction layer'') that moved along laterally right behind the oxidation front. They cited SEM data showing the segregated Sb layer lagging the oxidation front as evidence of a reaction layer with high amounts of dissolved Sb. The Sb layer lagged the oxidation front more at higher temperatures, suggesting a thicker reaction layer. Oxidation of elemental Sb is known to become quickly diffusion limited,[15] so they proposed that slow diffusion through the Sb-rich reaction layer could limit the oxidation at higher oxidation temperatures. Our SEM data also indicates a layer behind the oxidation front with different structure than the rest of the oxide that becomes wider and more distinct at higher temperatures. Therefore, we believe the same mechanism of slow diffusion through this layer is the most probable explanation for self-limiting oxidation in $AlAs_{0.1}Sb_{0.9}$. In any case, the same mechanism appears to be at work for both $AlAs_{0.56}Sb_{0.44}$ and $AlAs_{0.1}Sb_{0.9}$.

We are unsure of the role the Ga contamination may play in the oxidation kinetics. The Auger data in Fig. 6(b) shows that at this temperature, Ga comprises more than 10% of the column III content of the oxidized layer. It is clear that the Ga is incorporated into the $AlAs_{0.1}Sb_{0.9}$ layer as a result of a chemical process as opposed to thermal diffusion since the Auger profile of the unoxidized region (from the same sample) in Fig. 6(a) shows no Ga contamination. The Ga could have moved into the $AlAs_{0.1}Sb_{0.9}$ as a result of segregation of materials during oxidation of GaSb interfaces or through a chemical reaction of the GaSb interfaces with the oxide. It is known that the addition of 10% Ga to $AlAs_{0.56}Sb_{0.44}$ ($Al_{0.90}Ga_{0.10}AsSb$) during material growth can prevent oxidation of the material entirely at low temperatures.[9] We are currently investigating the effects of the Ga contamination in $AlAs_{0.1}Sb_{0.9}$ oxide.

Looking at how other compositions of $AlAs_xSb_{1-x}$ behave may lead to additional insights about self-limiting oxidation in $AlAs_{0.1}Sb_{0.9}$. For wet, thermal oxidation of pure AlAs, self-limiting oxidation does not occur; raising the oxidation temperature results in ever faster oxidation rates and greater oxidation depths.[14] In $AlAs_{0.56}Sb_{0.44}$, self-limiting oxidation limits oxidation depth for temperatures over 450 °C.[9] In $AlAs_{0.1}Sb_{0.9}$ studied here, self-limiting oxidation occurs above 340 °C. Finally, it is well known that AlSb readily hydrolyzes in atmospheric conditions at room temperature,[16,17] but Blum *et al.* reported that all their attempts to oxidize AlSb in a wet, thermal environment failed.[8] No mechanism for this strange behavior of AlSb oxidation was proposed. But we suggest that this behavior of AlSb may be the endpoint for onset of self-limiting oxidation behavior at lower temperatures as the Sb composition of $AlAs_xSb_{1-x}$ increases. Surface study of thermal oxidation of AlSb is called for to explore the anomalous behavior of AlSb, and maybe in the process shed light on oxidation kinetics of other $AlAs_xSb_{1-x}$ materials.

V. SUMMARY

In summary, lateral oxidation of $AlAs_xSb_{1-x}$ lattice matched to GaSb was investigated. A reasonable oxidation rate can be achieved at low temperatures, and lateral oxide progress up to 130 μm deep is easily realized. An oxidation rate of at least 2.15 μm/min was achieved at 350 °C, comparable to oxidation rates at this temperature that have been reported for oxidation of $AlAs_{0.56}Sb_{0.44}$ (Refs. 7 and 12) and much higher than those reported for oxidation of AlAs.[14] However, due to self-limiting oxidation, a tradeoff exists so that high oxidation rates and large maximum oxidation depths cannot be achieved at the same temperature. The oxidation starts off reaction rate limited, becoming diffusion rate limited for longer oxidation times and higher oxidation temperatures. Diffusion limited oxidation is accompanied by a change in oxidation front morphology, unlike in AlAs. The oxide is composed primarily of AlO_x and elemental Sb; the Sb exists as large grains near the center of the oxidized layer. SEM shows an interfacial layer right behind the oxidation front containing less segregated Sb than the rest of the oxidized layer that becomes more distinct with higher oxidation temperature. We believe that slow diffusion through this layer leads to self-limiting oxidation at high temperatures, analogous to the mechanism suggested by Mishra *et al.* for $AlAs_{0.56}Sb_{0.44}$.[9] We are currently exploring whether Ga contamination of the $AlAs_{0.10}Sb_{0.90}$ oxide from the surrounding GaSb layers may also play a role. Like $AlAs_{0.56}Sb_{0.44}$ the high content of elemental Sb in the oxide raises some concerns about the optical and electrical quality of the oxide, but otherwise we conclude that $AlAs_{0.1}Sb_{0.9}$ oxidation has much potential as a low-temperature processing tool for GaSb-based devices.

ACKNOWLEDGMENTS

The authors would like to thank Professor K. C. Hsieh for numerous fruitful discussions in the course of this research, and C. F. Xu for assistance with experiments. This work was partially supported by the U.S. Army Research Office MURI program (DAAD19-01-1-0591). SEM, AFM, and Auger depth profiling were carried out in the Center for Microanalysis of Materials, University of Illinois, which is partially supported by the U.S. Department of Energy under Grant No. DEFG02-91-ER45439.

[1] J. M. Dallesasse, N. Holonyak, Jr., A. R. Sugg, T. A. Richard, and N. El-Zein, Appl. Phys. Lett. **57**, 2844 (1990).
[2] A. Massengale, M. C. Larson, C. Dai, and J. S. Harris, Jr., Electron. Lett. **32**, 399 (1996).
[3] G. W. Pickrell, C. F. Xu, K. L. Chang, K. C. Hsieh, and K. Y. Cheng, J. Appl. Phys. **93**, 5429 (2003).
[4] K. D. Choquette, R. P. Schneider, M. Crawford Hagerott, K. M. Geib, and J. J. Figiel, Electron. Lett. **31**, 1145 (1995).
[5] O. Blum, K. M. Geib, M. J. Hafich, J. F. Klem, and C. I. H. Ashby, Appl. Phys. Lett. **68**, 3129 (1996).
[6] M. H. M. Reddy, D. A. Buell, A. S. Huntington, T. Asano, R. Koda, D. Feezell, D. Lofgreen, and L. A. Coldren, Appl. Phys. Lett. **82**, 1329 (2003).
[7] P. Chavarkar, U. K. Mishra, S. K. Mathis, and J. S. Speck, Appl. Phys. Lett. **76**, 1291 (2000).
[8] O. Blum, M. J. Hafich, J. F. Klem, K. Baucom, and A. Allerman, Electron. Lett. **33**, 1097 (1997).
[9] S. K. Mathis, K. H. A. Lau, A. M. Andrews, and E. M. Hall, J. Appl. Phys. **89**, 2458 (2001).
[10] A. M. Andrews and J. S. Speck, in *Proceedings of 2002 International*

Conference on Molecular Beam Epitaxy (IEEE, Piscataway, N.J., 2002), pp. 181–182.
[11] A. Salesse, R. Hanfoug, Y. Rouillard, F. Genty, G. Almuneau, L. Chusseau, A. Baranov, C. Alibert, J. Kieffer, E. Lebeau, and J. M. Luck, Appl. Surf. Sci. **161**, 426 (2000).
[12] P. Legay, P. Petit, G. Le Roux, A. Kohl, I. F. L. Dias, M. Juhel, and M. Quillec, J. Appl. Phys. **81**, 7600 (1997).
[13] M. Ochiai, G. E. Giudice, H. Temkin, J. W. Scott, and T. M. Cockerill, Appl. Phys. Lett. **68**, 1898 (1996).
[14] K. D. Choquette, K. M. Geib, H. C. Chui, H. Q. Hou, and R. Hull, Mater. Res. Soc. Symp. Proc. **421**, 53 (1996).
[15] A. J. Rosenberg, A. A. Menna, and T. P. Turnbull, J. Electrochem. Soc. **107**, 196 (1960).
[16] T. Shibata, J. Nakata, Y. Nanishi, and M. Fujimoto, Jpn. J. Appl. Phys., Part 1 **33**, 1767 (1994).
[17] Chin-An Chang, H. Takaoka, L. L. Chang, and L. Esaki, Appl. Phys. Lett. **40**, 983 (1982).